## Chapter 14

# Dispersion and Nucleating Effects of Clay Fillers in Nanocomposite Polymer Films

**Vincent Ferreiro, Gudrun Schmidt, Charles Han, and Alamgir Karim***

**Polymers Division, National Institute of Standards and Technology, Gaithersburg, MD 20899-8542**

Nanocomposite polymeric materials offer unique property advantages such as mechanical, electrical, thermal, etc. Such property enhancements are induced not only by the physical presence of the filler but also by the interaction of the polymer with the filler and the dispersion state of the filler. In the first section of the paper, we investigate the case of well dispersed laponite (synthetic clay) filler particles. Thin films cast from solutions of polyethylene-oxide (PEO)-laponite on glass substrates were prepared. Drying of the cast polymer-clay solutions produce transparent nanocomposite films and the laponite dispersion state appears to be trapped in the thin films. An optimal dispersion is obtained for a particular PEO/laponite ratio (r), that we find to be equal to $r \approx 0.66$. In a latter section of the paper, we investigate the case of weakly dispersed clay fillers. We find that weakly dispersed or "stacked" clay fillers can be used as nucleating agents ("seed" crystallization) in the crystallization of a clay-filled polymer blend (PEO / PMMA / Montmorillonite) film. As a function of increasing clay concentration, we make the novel observations that the number of dendritic branches increase substantially and tend to curl.





## Introduction

A recent upsurge of interest in polymer-clay nanocomposites due to their potential as low-cost materials with enhanced properties, has resulted in significant research into the synthesis and properties of nanocomposite materials[1-6]. However, much of this effort has been directed into measuring the bulk and solution properties and the chemistry of intercalation and exfoliation of the clay-fillers for forming such materials[7-9]. In contrast, the material properties of thin films of nanocomposite materials have not been explored to any significant extent. Nanocomposite thin films should pose interesting opportunities for exploiting property enhancements not only due to the available large polymer-clay surface area of contact, but also from geometric confining factors that induce a preferred orientation of the clay platelets relative to the film surface. Such an orientation may generate unique property enhancements like gas and vapor barrier properties in membranes of these materials. However, there have been very few reports on effects of preparation on dispersion and properties of thin nanocomposite films with a film thickness in the micrometer to nanometer scale range. We investigate nanocomposite films in this thickness range with the idea of studying dispersion effects on clay filled polymer film morphology and properties.

We first study the case of well dispersed Laponite (synthetic clay) filler particles. Thin films cast from solutions of polyethylene-oxide (PEO) -Laponite on glass substrates were prepared. Drying of the cast polymer-clay solutions produces transparent nanocomposite films and the Laponite dispersion state appears to be trapped in the thin films. An optimal dispersion is obtained for a particular PEO/Laponite ratio (r), $r \approx 0.66$ for the range of $0.33 < r < 1.66$. We next investigate the crystallization of a clay-filled polymer blend (PEO/PMMA/Montmorillonite) using the nucleating character of weakly dispersed clay fillers. Previous work[10] has shown that the surface enrichment of one blend component about the particles leads to a *counter enrichment* of the other phase about the first layer. This wave-like pattern of composition about the filler particles is probably important for stimulating crystallization about the clay particles. We find interesting dendritic patterns as a function of clay content.

## Experimental

### *PEO/Laponite Films preparation*

The synthetic hectorite type clay, Laponite, LRD, was provided by Laporte Industries Ltd[11]. The clay particles are composed of platelets of high purity and

uniform crystallite size[12,13]. In an aqueous medium, the clay forms transparent dispersions of disk shaped particles ca. 300 Å in diameter and ca. 10 Å thick[12,13] Poly(ethylene-oxide) with a $M_w$ = 1,000,000 g/mol was purchased from Polysciences Inc.[11]. Various concentrations of LRD and PEO were prepared in distilled deionized water and mixed for at least 2 weeks (Table 1). The pH and ionic strength of the solutions were controlled by the addition of NaOH and NaCl, respectively. For all samples in this study a pH value of 10 and a NaCl concentration of $10^{-3}$ mol/L were used. Under these conditions a flocculation due to the dominance of van der Waals attraction over electrostatic repulsion of the clay particles is avoidable[14]. LRD, LRD2, LRD5 solutions were cast on glass slides and dried at 25 °C for 24 h under vacuum. Transparent films with an average thickness of 5 μm were obtained by spreading the filled polymer solution on a glass substrate with a blade. The surface morphology and the roughness of these films have been characterized by AFM.

**Table1. PEO/Laponite Film Characteristics**

| sample | PEO mass fraction, % PEO in solution ($D_2O$) | PEO mass fraction, % PEO in dried films | LRD mass fraction, % LRD in solution ($D_2O$) | LRD mass fraction, % LRD in dried films |
|---|---|---|---|---|
| LRD | 0 | | 3 | |
| LRD2 | 2 | 40 | 3 | 60 |
| LRD5 | 5 | 62.5 | 3 | 37.5 |

*PEO/PMMA/Montmorillonite Films Preparation*

"Cloisite" (Montmorillonite; MON) clay particles were obtained from Southern Clay Products[11]. This clay mineral has exchangeable sodium ions, and a cation exchange capacity of ca. 95 meq (milli-equivalent) per 100 g. PEO with average $M_w$ = 200,000 g/mol and PMMA of $M_w$ = 120,000 g/mol were purchased from Aldrich, USA. MON (1 g) and 50 ml of distilled water at 80°C were placed in 0.1L beaker, and 1 g of distearyldimethyl ammonium chloride was added to the solution. The mixture was stirred vigorously for 1h, then filtered and rinsed three times with 100 ml of hot water to remove NaCl. After being washed with ethanol (50 ml) to remove any excess of ammonium salt, the product was freeze-dried, and kept in a vacuum oven at room temperature for 24 h. The resulting organically modified montmorillonite (OMON) dispersed well in chloroform, although the unmodified montmorillonite (MON) did not disperse. The blend components (PEO/PMMA/OMON) were dissolved in chloroform at a total mass fraction of 1%, unless otherwise stated. Thin blend films were spin coated onto Si substrates (Semiconductor Processing Co., orientation (100), Type P) at a spin speed of 2000 rounds per minute (rpm). This procedure results in films having a uniform thickness of ≈ 200 nm. Prior to spin coating, the Si wafers were "piranha-etched" to form a native $SiO_2$ surface layer.

*Film Morphology Characterization*

Reflective optical images were obtained with an optical microscope (OM) using a Nikon optical microscope with a digital Kodak MegaPlus CCD camera attachment.

All AFM experiments were carried out in air using a Dimension 3100 microscope from Digital Instruments operating in the Tapping mode™ [11]. In this mode, the cantilever is forced to oscillate at a frequency close to its resonance frequency with an adjustable amplitude. The tip, attached to the cantilever, was a pure silicon single crystal tip (model TSEP) with a radius of curvature of about 10 nm. The tip contacts briefly the film surface at each low position of the cantilever and the amplitude of the oscillation varies. "Height" images are obtained by using the feedback loop that keeps the amplitude at a constant value by translating vertically the sample with the piezoelectric scanner: height measurements are deduced from those displacements. For the engagement we used a ratio $A_{sp}/A_o = 0.9$, where $A_o$ is the free oscillation amplitude and $A_{sp}$ the set-point one[15,16]. Besides the variation of the amplitude, the dephasing of the cantilever oscillation relative to the signal exciting the piezoelectric driver can be measured: that mode is called "Phase Detection Imaging" (PDI)[17-19] and is usually used to probe local elastic or adhesive properties at the surface. However, in our system, the dynamic force curves show that the phase images do not reveal any difference of mechanical properties between the matrix (PEO) and the fillers. Only, topographic features have been observed, using a ratio $A_{sp}/A_o = 0.8$ which provides a better image contrast. Roughness analyses were also performed on some samples, conducted according to the manufacturer's software program. The root-mean-square (RMS) average of the surface roughness value was calculated as the standard deviation of all the height values within the given area.

**Results and Discussion**

*PEO-Laponite Films*

Upon drying, the polymer clay solutions produce transparent nanocomposite films with micro-porous membrane character and elastic properties. These films

(thickness ≈ 5 μm) were cast from solutions containing 95 % water by mass. We expect that AFM of the dried film may even provide insights into the network character of the polymer in solution. Most reinforcing agents, such as fibers and fillers are large and scatter light, thus reducing light transmittance. Efficient particle dispersion combined with good interfacial adhesion is achieved in the aqueous polymer clay solution and this property is maintained in the film. This is the main reason for transparency. From a practical viewpoint, this allows the exiting possibility of developing strong yet transparent films, coatings and membranes from solution.

AFM images of the pure LRD film (Table 1) are displayed in Figure 1, illustrating the size and orientation of the structured nanoparticles. For comparison the height and phase image of the LRD sample (Figure 1a and 1b) show clay particles which lie flat on the surface. However the RMS roughness of the film is equal to ≈ 12 nm. An arrow in the insert of Figure 1c points to a single platelet. The average diameter of the clay platelets is about 30 nm which is consistent with previous SANS[20] experiments and published literature[21-23]. By drying LRD2 we obtain a film with clay particles which are randomly oriented and connected by polymer (Figure 2 a-b). LRD5 dried films exhibit two areas with quite different representative structures (Figure 2 c-d). The first structure is a mesoporous homogeneous film texture with same size particles.

The second structure is a heterogeneous one and contains: 1) domains where only excess PEO is observed (black arrow in Figure 2 c-d) and 2) areas where clay particles are agglomerated (white arrow). In both cases the polymer acts as a connection between particles. LRD2 produces an elastic porous film with clay particles, which are covered and connected by polymer and randomly oriented (Figure 2b). We notice that the RMS roughness of these films decreases with increasing PEO concentration showing that the network produces a smoother surface than the LRD film (RMS roughness (LRD) = 12 nm and RMS roughness (LRD2 and LRD5) ≈ 5 nm. LRD2 dried films exhibit spherically particles with each particle having the same average diameter compared to one clay platelet (Figure 2b).

In contrast to LRD2, some areas of LRD5 films show domains with excess of PEO These domains are the white "dots" in Figure 2 c-d. LRD5 solutions studied by SANS and flow birefringence[20] show exfoliated clay particles and well dispersed PEO. AFM investigations of LRD5 dried films show that this composition appears to be the critical concentration where a transition from a homogeneous network like structure to a heterogeneous structure occurs. The excess PEO does not contribute to building the network. A more detailed study around this critical concentration will be made in the future. With increasing PEO mass fraction beyond a value of 5 % in a solution, the number and the size of PEO "dots" in a dried film increases, and no isolated clay platelet can be observed since the clay platelets are all polymer covered. In all cases the polymer provides strong connections between clay particles as has been shown by

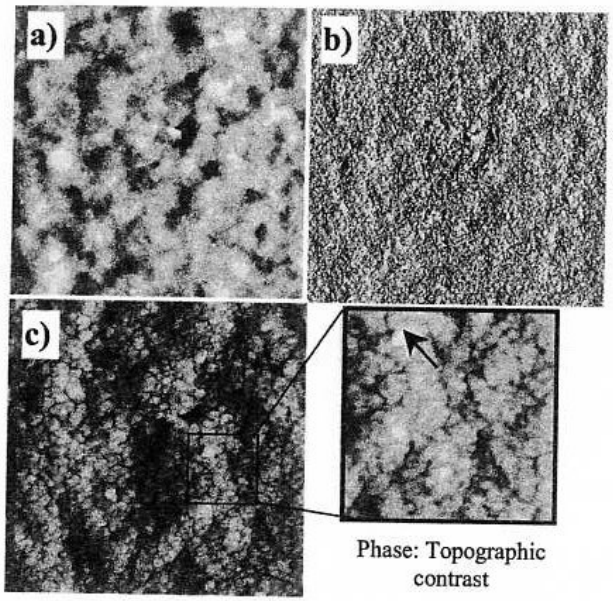


***Figure 1.*** *AFM images of LRD film morphology without PEO*

*a). "Height" AFM image (3 μm x 3 μm) of LRD film , Z range = 48 nm*

*b). "Phase" AFM image (3 μm x 3 μm) of LRD film, Phase = 34°.*

*c). On the top right corner a zoom of Fig. 1b show clay flat on with a average diameter of 30 nm (300 nm x 300 nm), Phase = 55°*

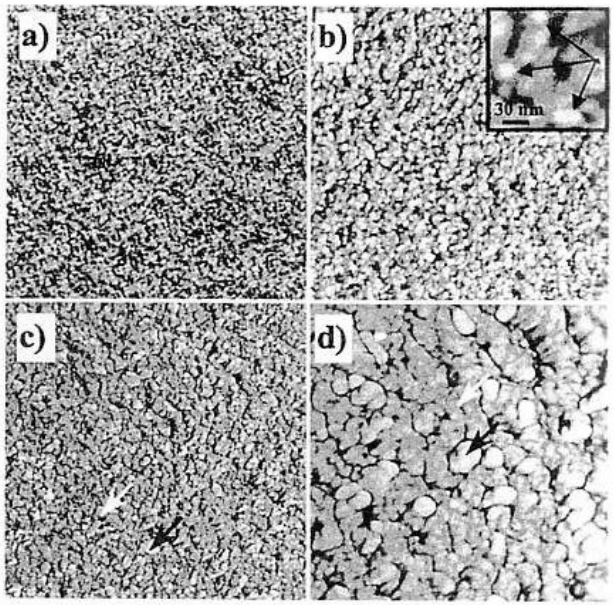


*Figure 2. AFM images show the evolution of LRD film morphology as a function of PEO/clay ratio (r)*

***a).*** *"Phase" AFM image (3 μm x 3 μm) of LRD2 film (r = 0.66), Phase = 126°* ***b).*** *"Phase" AFM image (1 μm x 1 μm) of LRD2 film (r = 0.66), Phase = 45° (Zoom of Fig. 2a). On the top right corner a zoom of the network is shown (1 μm x 1 μm), phase = 69°. We can see three clay platelet flat on and separated from each other with the same distance.* ***c).*** *"Phase" AFM image (3 μm x 3 μm) of LRD5 film (r = 1.66), Phase = 111°.* ***d).*** *"Phase" AFM image (1 μm x 1 μm) of LRD5 film (r = 1.66), Phase = 106° (Zoom of Fig. 2c) showing the PEO in excess and the agglomerated clay particles.*

rheology experiments[20]. Moreover, after annealing the films at 50 °C or after isothermal crystallization in order to crystallize the PEO, no morphological modifications were observed. Additional DSC experiments on LRD2 samples show no crystallization peak in the range of (30 to 200) °C. However LRD5 shows a peak at ≈ 60 °C. While it is possible to form polymer microcrystals inside LRD5, there is not enough PEO chain mobility to crystallize LRD2 because of the strong interactions with the clay fillers within the network. Upon annealing far above the melting temperature of PEO ($T_m$ = 71 °C) both films show no dewetting and are stable for hours suggesting there is no degradation of the polymer or film properties.

Preliminary SANS results on both samples show no significant temperature dependence up to 100 °C. However strong concentration dependence was detected ($0.03\ nm^{-1} > q > 0.3\ nm^{-1}$), which may be correlated with the morphology as observed in AFM. The clay seems to be completely exfoliated since SANS data show no peaks which would be expected for clay packets.

*PEO/PMMA/OMON Films*

As a second part of the study, we investigate the case where the clay fillers are weakly dispersed. In this case, we have shown in a previous paper that the clay plays the rule of nucleating agents for the crystallization of the PEO. The morphology of polyethylene oxide (PEO) crystallization in a thin film geometry can be "tuned" through spherulitic, seaweed, dendritic and DLA-like crystallization forms through the adjustment of PEO composition and the degree of supercooling. Figure 3 shows the polymer dendrites in a (30/70) mass ratio (PEO/PMMA) blend. The dark features (≈ 1 μm in size) in the optical micrograph correspond to agglomerate clay particle which "seed" the crystallization. The diameter of the clay particle found by TEM on a cast solution OMON/chloroform on copper grid is ≈ 100 nm as we can see in Fig. 4.

*Effect of Temperature and Clay mass concentration on Blend Crystallization Morphology.*

After spin-casting, the films were heated to 100 °C for 5 min. in order to melt the PEO. The films are then cooled down to the desired crystallization temperature. PEO/PMMA films were crystallized at different temperatures[25]. The film thickness was approximately constant (h = 150 nm) and the clay content was 5 % of the polymer blend mass. A nearly square (equilibrium crystallization) crystal forms for low undercooling (10 °C) and we observe a change to a

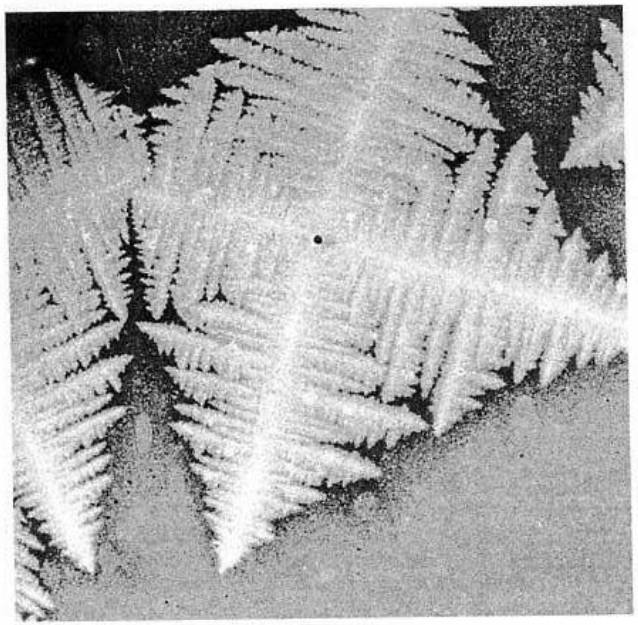

***Figure 3.*** *Symmetric dendritic morphology of a (30/70) PEO/PMMA blend film crystallized at 32 °C during 2 h. Optical image shows the regular "star-like" morphology of the dendrites.*

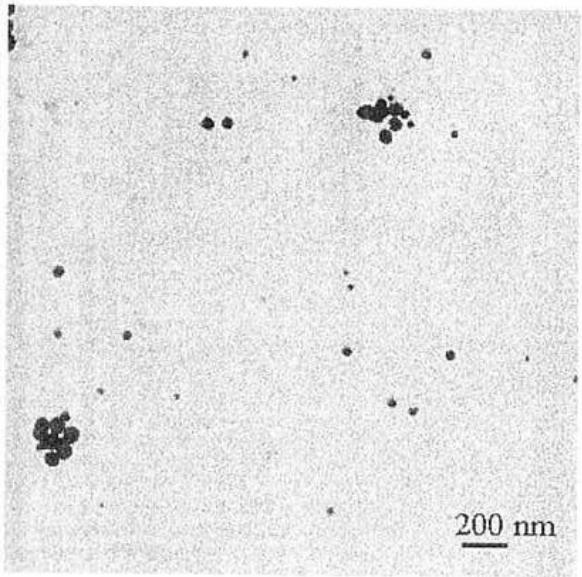


***Figure 4.*** *Transmission Electron Microscopy of a dried Clay/Chloroform solution on copper grid. We found a diameter value of the Montmorillonite clay particles between 50 nm and 100 nm.*

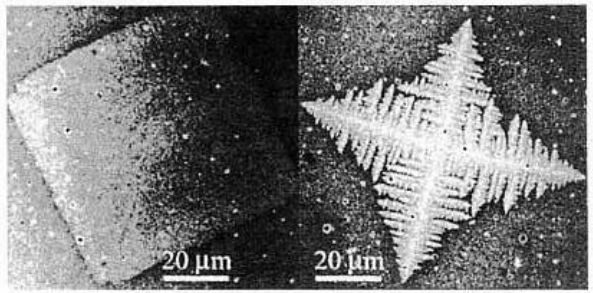


***Figure 5.*** *Parameters influencing the morphology of PEO/PMMA blend. Optical images showing the evolution of the dendrite morphology with the degree of undercooling.*

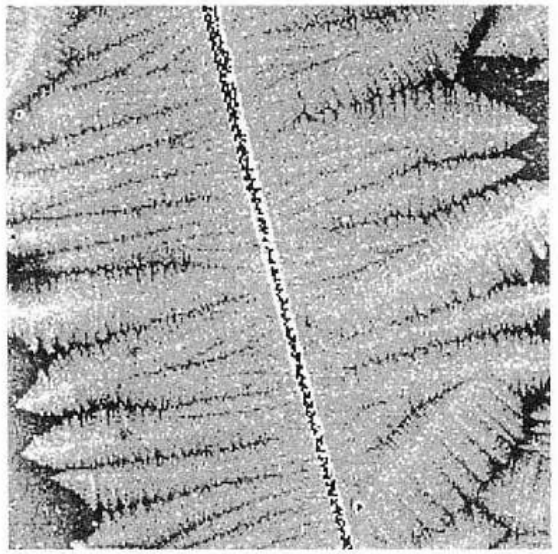

***Figure 6.*** *Optical image showing a dendritic wavefront propagating perpendicularly to a scratch. Crystallization conditions are the same as in Fig. 3, except there is no clay added to the polymer.*

dendritic morphology at high undercooling (35 °C) (Fig. 5) Under identical crystallization conditions (polymer composition, temperature, film thickness) there are no crystallization patterns in the absence of clay particles to nucleate the crystallization. The films are "excitable", however, and scratching a (30/70) PEO/PMMA blend film induces the formation of a dendritic wavefront that propagates to cover the film (Fig. 6). Dust particles were also observed to initiate dendrite growth in PEO/PMMA blend films without the clay filler. We then see that film imperfections can have a large influence on the properties of semi-crystalline blend films.

Adding clay particles can induce other effects than simply nucleate the polymer crystallization. At higher clay content (> 5 %), the interference between competiting growth centers (nucleating clay sites) can cause the dendrite arms to further branch, leading to dendrites with an increased numbers of arms. We illustrate this effect in Fig. 7 for a mass fraction of 10 % clay where the relative PEO/PMMA blend composition is again fixed at (30/70). At clay content below 5 %, we only observe dendrites having four arms (See Fig. 3). We also showed in a separate paper that increasing clay particle concentration causes the arm of the dendrite to curl[25].

There are no dendrites formed in the blend films without clay or film imperfections (scratches). The local compositional enrichment caused by the clay or defects then appears to be important for nucleating polymer dendrites. There is a subtlety to this heterogeneous nucleation process that was not originally anticipated in the planning of our measurement. The clay particles are nearly spherical in shape [average radius, R ≅ 100 nm)] and have been treated with surfactant to facilitate their dispersal in the polymer blend. We find that the clay particles do not disperse in the pure PEO, but rather segregate to the polymer-air boundary. The PEO films recrystallize into spherulites and appear similar to films without clay. This leads us to the question of how the clay particles could serve to nucleate crystallization in the PEO/PMMA blend. Previous work[1] has shown that the surface enrichment of one blend component about the particles leads to a *counter enrichment* of the other phase about the first layer. This wave-like pattern of composition about the filler particles is probably important for stimulating crystallization about the clay particles. Thus, it is not necessary for an effective nucleating agent to have a favorable interaction with the crystallizing species in a polymer blend.

In summary, we have shown that depending on the preparation of the thin films, whether the clay fillers are well dispersed or weakly dispersed can lead to substantially modifying the morphology and properties of the films. We also found that in the case of mixing clay with a semi-crystalline polymer, the agglomerated clay fillers can act as nucleating agents for seeding crystalline structure.

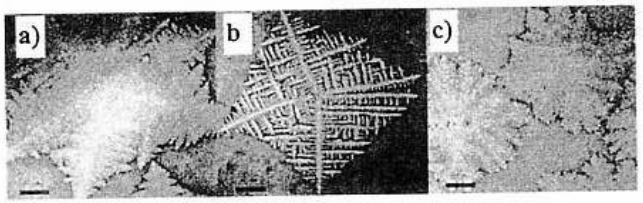


***Figure 7.*** *Optical image showing the increase of dendrite branches with the clay mass fraction of polymer. a) 10 %, b) 15 % and c) 20 %.*

**Acknowledgements**

We thank Jack Douglas for useful discussions related to the paper. Gudrun Schmidt acknowledges financial support by the Alexander von Humboldt foundation.

**References and Notes:**

1. A. Usuki, M. Kawasumi, Y. Kujima, A. Okada, *J. Mater. Res.*, **8**, 1174 (1993);
2. Y. Kojima, M. Kawasumi, A. Okada, Y. Fukushima, T. Kurauchi, O. Kamigatio, *J. Mater. Res.*, **8**, 1179 (1993);
3. A. Okada, A. Usuki, *Mater. Sci. Eng: C*, **3**, 109 (1995);
4. T. Lan, T. Pinnavaia, *J. Chem. Mater.* **6**, 2216 (1994);
5. Z. Wang, T. Pinnavaia, *J. Chem Mater.* **10**, 1820 (1998);
6. K. Yano, A. Usuki, A. Okada, T. Kurauchi, O. Kamigaito, *J. Polym. Sci. A: Polym. Chem.* **31**, 2493 (1993);

7. K. Yano, A. Usuki, A. Okada, *J. Polym. Sci.: Part A: Polym. Chem.* **35**, 2289 (1997);
8. R. Krishnamoorti, E.P. Giannelis, *Macromol.* **30**, 4097 (1997);
9. Intercalation Chemistry, Whittingham M.S., Jacobson A.J.. eds., Academic Press, New York, 1992;
10. B.P. Lee, J.F. Douglas, S.C. Glotzer, *Phys. Rev. E* **60**, 5812 (1999);
11. Certain equipment and instruments or materials are identified in this paper in order to adequately specify the experimental details. Such identification does not imply recommendation by the National Institute of Standards and Technology nor does it imply the materials are the best available for the purpose;
12. J.D.F. Ramsay, S.W. Swanton, J.Bunce, *Chem. J. Soc. Faraday Trans.* **86**, 3919 (1990);
13. F. Pignon, A. Magnin, J.M. Piau, B. Cabane, P. Lindner, O. Diat, *Phys. Rev. E.* **3**, 3281 (1997);
14. J.M. Saunders, J.W. Goodwin, R.M. Richardson, B. Vincent, J. Phys. Chem. B **103**, 9211 (1999);
15. R. Boisgard, D. Michel, J.P. Aimé, *Surf Sci.* **401**, 199 (1998);
16. J.P. Aimé, D. Michel, R. Boisgard, L. Nony, *Hys Rev B.* **59**,1829 (1999);
17. S.N. Magonov, V. Elings, M.H. Wangbo, *Surf Sci.* **389**, 201 (1997);
18. S.N. Magonov, J. Cleveland, V. Elings, *Surf Sci.* **375**, 385 (1997);
19. D. Michel, *PhD thesis*, (1997), Université de Bordeaux 1, France;
20. G. Schmidt, A.I. Nakatani., P.D. Butler, A. Karim, C.C. Han, *Macromolecules.***33,** 7219 (2000);
21. A. Mourchild, A. Delville, J. Lambard, E. Lecolier, P. Levitz, *Langmuir* **11**, 1942 (1995);
22. J.H.M. Hanley, G. Straty, *Langmuir*, **10**, 3362 (1994);
23. F. Pignon, A. Magnin, J.M. Piau, *J. Rheol.* 42, **6**, 1349 (1998);
24. V. Ferreiro, J. Douglas, E.J. Amis, A. Karim, in press *ACS Proceeding* (2000);
25. V. Ferreiro, J. Douglas, J. Warren, A. Karim, submitted.

Reprinted from ACS Symposium Series 804
Polymer Nanocomposites
Synthesis, Characterization, and Modeling
Ramanan Krishnamoorti, Richard A. Vaia, Editors
Published 2001 by the American Chemical Society